

## Response Mechanism of a Molecular Recognition Ion Gating Membrane

Taichi Ito, Yuya Sato, Takeo Yamaguchi,\* and Shin-ichi Nakao

Department of Chemical System Engineering, The University of Tokyo,  
7-3-1 Hongo, Bunkyo-ku 113-8656, Japan

Received December 30, 2003; Revised Manuscript Received February 24, 2004

**ABSTRACT:** A molecular recognition ion gating membrane opens and closes its pores using the volume phase transition of PE (polyethylene)-*g*-*N*-isopropylacrylamide (NIPAM)-*co*-benzo[18]crown-6-acrylamide (BCAm), which recognizes specific ions with its BCAM receptors and changes its volume by swelling and shrinking. In this study, we clarify the mechanism of the molecular recognition response of the PE-*g*-NIPAM-*co*-BCAM. The complex formation constant ( $\log K$ ) of the crown ether receptors contained in BCAM units was determined to be an order of magnitude lower than that of benzo[18]crown-6. Calculating from  $\log K$ , we estimated the quantity of the complex of the crown ether receptor and the ion; the ratio of the BCAM units forming the complex to total monomer units that consists of NIPAM and BCAM ( $X$ ) was below 5%. Although  $X$  was less than 5%, the complex affected the swelling and the shrinking of NIPAM units. Poly-NIPAM is well-known to change its volume at the lower critical solution temperature (LCST), being accompanied by the change of the enthalpy ( $\Delta H$ ). The differential scanning calorimetry (DSC) data of PE-*g*-NIPAM-*co*-BCAM showed that LCST increased and  $\Delta H$  decreased with increasing  $X$ , regardless of ion species.  $\Delta H$  is generated to compensate for the breakage of hydrogen bonds between the water molecules that surround the hydrophobic moieties of polymer chains; therefore, formation of the complexes of the crown ether receptors and the ions broke the hydrogen bonds and then shifted the LCST higher. In addition, the LCST determined by DSC predicts the temperature at which the membrane pores open. Therefore, this suggested mechanism contributes to both the molecular design of grafted stimuli-responsive copolymers and the design of the gating membrane function.

## Introduction

Some gating membranes<sup>1</sup> that control their own permeabilities in response to stimuli such as temperature, pH, light, and molecular signal have been developed. By mimicking the gating function of the ion channels of biomembranes, we have developed molecular recognition ion gating membranes.<sup>2–4</sup> These gating membranes can control solvent flux,<sup>2</sup> solute rejection,<sup>3</sup> or diffusivity<sup>4</sup> in response to specific ion signals. However, the design principle and mechanism of our gating membrane were unique and quite different from those of the ion channels of biomembranes.

Our molecular recognition ion gating membrane has the grafted copolymer of *N*-isopropylacrylamide (NIPAM) and benzo[18]crown-6-acrylamide (BCAM) on its pore surface, as shown in Figure 1. These two monomer units have different roles. NIPAM swells below its lower critical solution temperature (LCST) and shrinks above its LCST, dramatically releasing any free water<sup>5</sup> with the change of the enthalpy ( $\Delta H$ ).<sup>9,10,12–16,22</sup> It acts as an actuator by its volume change. BCAM has a crown ether receptor, which captures a specific ion selectively. It acts as a sensor. Thus, the LCST of the copolymer of NIPAM and BCAM shifts when the receptors of crown ethers of BCAM capture the specific ions, as shown in Figure 2.<sup>6</sup> Consequently, the copolymer swells and shrinks at a constant temperature located between the two LCSTs in response to Ba<sup>2+</sup> or K<sup>+</sup> ions. When the grafted copolymer swells in the substrate pores in response to Ba<sup>2+</sup> or K<sup>+</sup> ions, the swelling grafted copolymer fills the pores, and then the pores close. On the other hand, when the grafted copolymer shrinks by releasing Ba<sup>2+</sup> or K<sup>+</sup> ions, the center of the pores becomes hollow because the grafted copolymer exists near the substrate

pore surface. Then, the pores open. As shown in our previous paper,<sup>2,3</sup> the thickness, the pore size, and the porosity of the used substrate were 110  $\mu\text{m}$ , 0.2  $\mu\text{m}$ , and 0.69, respectively. In addition, the copolymer was grafted onto the only pore surface near the membrane surfaces. Thus, this pore size change occurred only near the pore surface.

To clarify the response mechanism of the gating membrane, an understanding of the phase transitions of the copolymer of NIPAM and BCAM is essential, as the shrinking and swelling of the grafted copolymer causes the opening and closing of the gating membrane. Some copolymers that contain both a sensor and an actuator have been reported in previous studies, e.g., the copolymer of NIPAM and boronic acid monomer<sup>7</sup> in response to glucose concentration, and that of NIPAM and a monomer containing antibody<sup>8</sup> in response to antigen is well-known. The understanding of poly-NIPAM-*co*-BCAM will also contribute to understanding and designing copolymers containing both an actuator and a sensor in general.

A previous study reported that the phase transition of hydrogel of NIPAM occurs with hydration and dehydration. To clarify the hydration around poly-NIPAM or copolymers of NIPAM and functional group pendant monomers, infrared (IR) spectroscopy,<sup>9,11</sup> differential scanning calorimetry (DSC),<sup>9,10,12–16,22</sup> nuclear magnetic resonance (NMR),<sup>15,17</sup> Raman spectroscopy,<sup>18</sup> and fluorescence spectroscopy<sup>19</sup> have been used in previous studies, with DSC being frequently used because DSC measurements can determine both LCST and  $\Delta H$ . LCST is normally defined as the temperature at the peak or the onset of the DSC thermogram, and  $\Delta H$  is normalized to be divided by the molar quantity of monomer units in the polymer. Maeda et al.<sup>9</sup> carried out a DSC study on a copolymer of NIPAM and sodium styrenesulfonate (SSNa), which has a charged functional group. The peak of the DSC thermogram broad-

\* Corresponding author: e-mail yamag@chemsys.t.u-tokyo.ac.jp;  
Tel +81-3-5841-7345; Fax +81-3-5841-7227.

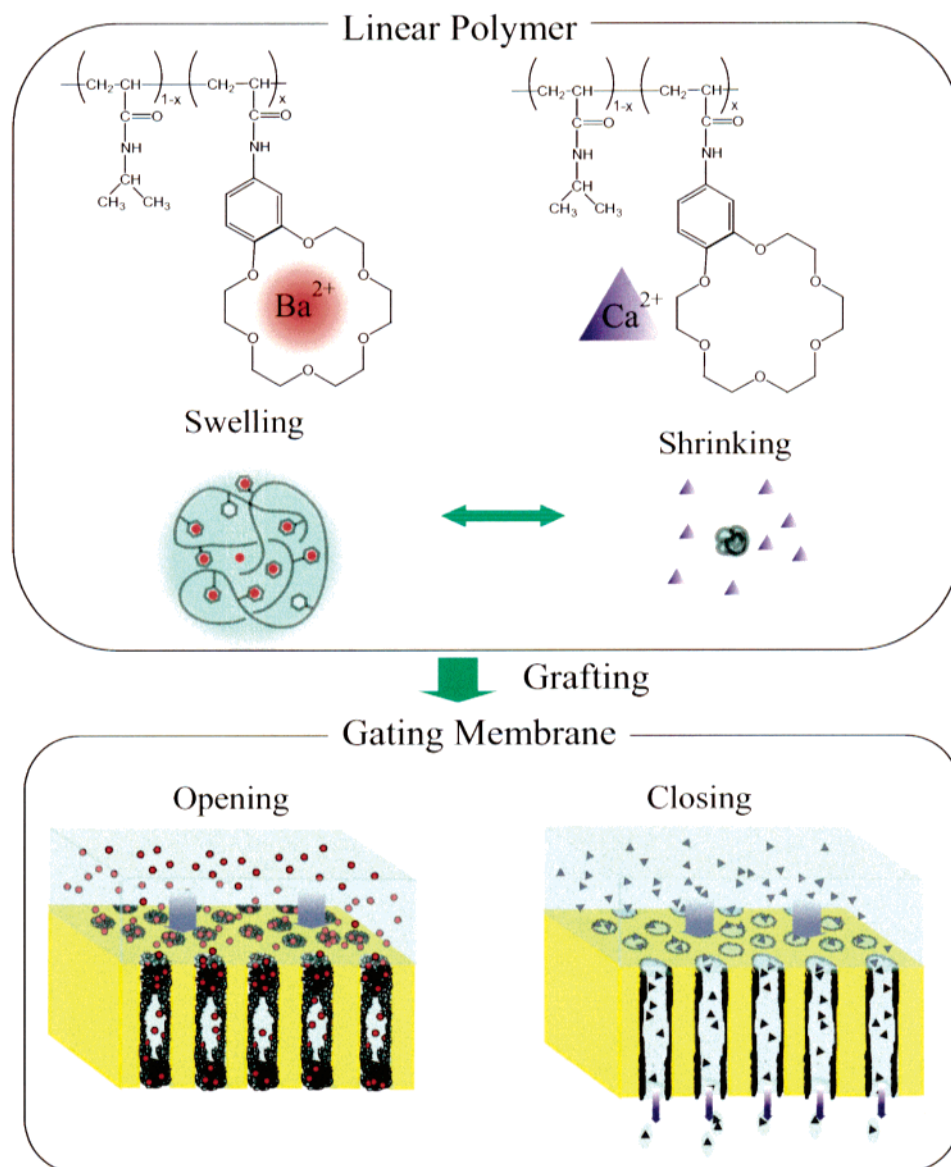


**Figure 1.** Schematic representation of PE-*g*-NIPAM-*co*-BCAm. The copolymer of the thermosensitive polymer, NIPAM, and the crown ether polymer, BCAM, is grafted onto a high-density polyethylene (HDPE) surface. The polymer senses a specific ion,  $M^{m+}$  with its crown ether receptor, and then swells.

ened and  $\Delta H$  decreased with an increasing proportion of SSNA in the copolymer. This means that the introduction of a charged functional group influenced the water structure in the hydrogel and changed LCST and  $\Delta H$ . To clarify the mechanism of the phase transition of the copolymer of NIPAM and BCAM, we must also consider the hydration of the copolymer chain of NIPAM and BCAM. In particular, the ions captured by the receptors of BCAM might influence the hydration of the grafted copolymer of NIPAM and BCAM; thus, we must investigate the effect of the captured ion on the hydration of the copolymer.

The aim of our study was to clarify the mechanism of the molecular recognition response of the gating membrane. To achieve this, it was necessary to clarify the response mechanism of the copolymer of NIPAM and BCAM. The important factors are (i) the quantity of crown ether receptors, (ii) the complex formation constant of the crown ether receptors, and (iii) the relationship between hydration of the grafted copolymer and the ions captured by the crown ether receptors. First, the quantity of crown ether receptors included in both

the linear copolymer and the grafted copolymer of NIPAM and BCAM was determined by spectroscopic methods such as IR and ultraviolet (UV). Second, the complex formation constant of the copolymer,  $\log K$ , was determined by both ion adsorption experiments using a conductometric analyzer and ion mobility measurements using an impedance analyzer. Finally, the relationship between the complex formation ratio and the enthalpy of the phase transition ( $\Delta H$ ) was clarified using DSC.

## Experimental Section

**Preparation of PE-*g*-NIPAM-*co*-BCAm and the Poly-NIPAM-*co*-BCAm.** BCAM was synthesized according to reported procedures.<sup>20</sup> Both NIPAM and BCAM were recrystallized from benzene.

Polyethylene (PE)-*g*-NIPAM-*co*-BCAm was prepared by peroxide plasma graft polymerization.<sup>2,3</sup> For monomer solutions, a mixture of NIPAM and BCAM and water was emulsified with sodium dodecyl sulfate (SDS). Both the SDS and the total monomer concentration in solution were fixed at 4 and 5 wt %, respectively. The weight percentage of BCAM in the

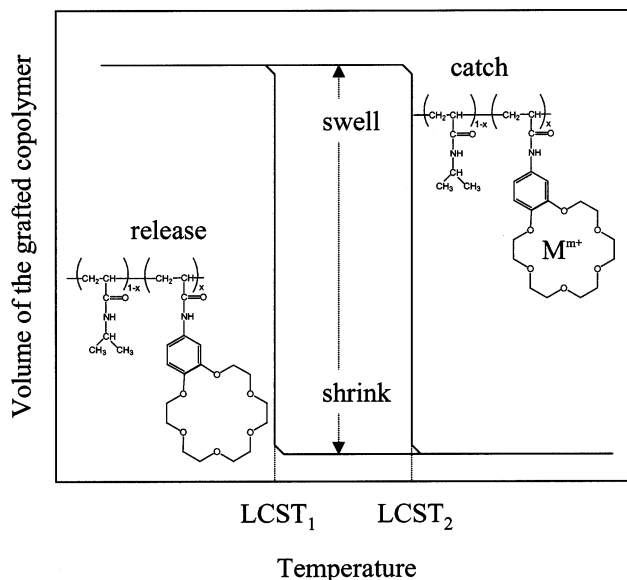


**Figure 2.** Schematic illustration of the volume change of the NIPAM/BCAm copolymer. On capturing a specific ion, this copolymer changes its LCST from  $LCST_1$  to  $LCST_2$ ; thus, the copolymer swells and shrinks in response to the presence of  $M^{m+}$  between  $LCST_1$  and  $LCST_2$ .

monomers was fixed at 15 wt %. A porous high-density polyethylene (HDPE) film was used as a substrate. The thickness, the pore size, and the porosity of the substrate were 110  $\mu\text{m}$ , 0.2  $\mu\text{m}$ , and 0.69, respectively. The substrate was irradiated with argon plasma to form initiator radicals, using a plasma power of 10 W and treatment period of 60 s. Following the plasma treatment, the plasma-treated substrate was left in contact with the air for 60 s. After air contact, the monomer solution was introduced by immersing the treated substrate; this was then heated to 80  $^{\circ}\text{C}$ . PE-*g*-NIPAM that did not contain any BCAM was prepared using plasma activation graft polymerization.<sup>21</sup> The amount of grafted polymer,  $W$ , is defined as follows:

$$W[\text{mg}/\text{cm}^2] = \frac{W_2 - W_1}{A}$$

where  $W_1$  is the weight of HDPE substrate before polymerization,  $W_2$  is the weight of HDPE substrate after polymerization, and  $A$  is the area of the HDPE substrate.

Poly-NIPAM-*co*-BCAm was synthesized using radical copolymerization in distilled tetrahydrofuran (THF) using 0.3 mol % azobis(isobutyronitrile) (AIBN) as initiator at 70  $^{\circ}\text{C}$  according to the method used previously.<sup>21</sup> The molar ratio of NIPAM to BCAM in the monomer solution was 95:5, which is equal to 85:15 as a weight ratio. The concentration of the monomer solution was 25 wt %. Poly-NIPAM and poly-BCAm were also synthesized using radical polymerization in dehydrated *N,N*-dimethylformamide (DMF) using 1.0 mol % AIBN. All of the synthesized polymers were purified by reprecipitation from diethyl ether.

**Spectroscopic Measurements.** The synthesized grafted and linear polymers were characterized by spectroscopic measurements, such as IR and UV-vis spectroscopy. The IR spectra of PE-*g*-NIPAM, poly-NIPAM-*co*-BCAm, poly-BCAm, and poly-NIPAM were measured using the KBr disk technique with a MAGNA550 (Nicolet). The UV-vis spectra of poly-NIPAM-*co*-BCAm and poly-BCAm were measured using a U-3310 (Hitachi). The absorption intensities of UV spectra were measured in polymer aqueous solutions of concentrations below  $1.2 \times 10^{-4}$  M.

**Measurement of Adsorbed Ions.** The concentrations of  $\text{K}^+$  adsorbed by the receptors of PE-*g*-NIPAM-*co*-BCAm in a mixture of water and methanol were measured. For the adsorption solution, KCl was dissolved in a mixture of methanol and water. The concentration of these salts varied between

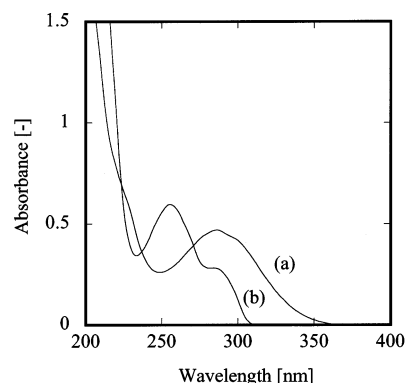


**Figure 3.** UV spectra of (a) poly-BCAm and (b) poly-NIPAM-*co*-BCAm.

0.675 and 40 mM. The weight ratios of methanol to water were 100, 90, and 70 wt %. The procedure for the adsorption measurements was as follows. PE-*g*-NIPAM-*co*-BCAm was washed in pure solvent mixture at least four times to desorb the ions. After washing, PE-*g*-NIPAM-*co*-BCAm was shaken in the prescribed KCl solution for 30 min at 25  $^{\circ}\text{C}$ . Finally, the KCl concentration of the solution was calculated from the electrical conductivity measured, using a CM-50AT (DKK-TOA Co.).

**Ion Mobility Measurements Using an Impedance Analyzer.** The ionic mobility of poly-NIPAM and poly-NIPAM-*co*-BCAm aqueous solution was measured using an impedance analyzer. The polymers were dissolved in distilled pure water by stirring and ultrasonication; the concentrations of the polymer varied between 0 and 0.16 wt %. To these polymer aqueous solutions, KCl,  $\text{SrCl}_2$ , or  $\text{BaCl}_2$  was added at a fixed concentration of 0.10 M. The ionic mobility of the prepared polymer aqueous solution was measured at 25  $^{\circ}\text{C}$  using an impedance analyzer (4192A; Hewlett-Packard).

**DSC Measurements.** LCST and  $\Delta H$  of PE-*g*-NIPAM-*co*-BCAm were measured using a DSC. A PE-*g*-NIPAM-*co*-BCAm film was cut into a disk with a 5 mm radius. After immersion in methanol, 10 of these disks were washed in distilled pure water five times to exchange the solvent from methanol to water and to desorb ions.

After washing, the disk films were shaken in ionic aqueous solution for 30 min. For adsorbed ions, KCl, NaCl,  $\text{SrCl}_2$ , and  $\text{BaCl}_2$  were used; their concentrations varied between 5 and 500 mM. The disk films adsorbing the ions were placed in a sealed pan, which was heated from 25  $^{\circ}\text{C}$  to 55 or 60  $^{\circ}\text{C}$  at a heating rate of 5  $^{\circ}\text{C}/\text{min}$ . After heating, the samples were cooled at the same rate using a DSC-7 (Perkin-Elmer). The heating and cooling cycles were repeated three times; from those measured values, the values for the second heating run were used for analysis. LCST was defined as the temperature at the peak of the DSC thermogram, and  $\Delta H$  was normalized to be divided by the molar quantity of monomer units in the grafted copolymer.

## Results and Discussion

**Quantity of Crown Ether Receptors Contained in Poly-NIPAM-*co*-BCAm and PE-*g*-NIPAM-*co*-BCAm from Spectroscopic Measurement.** This quantity was measured by UV-vis. Figure 3 shows the UV spectra of poly-NIPAM-*co*-BCAm and poly-BCAm, which had an absorbance peak at 255 nm. The following proportional relationship existed between the absorbance at 255 nm and the concentration of poly-BCAm:

$$C_{\text{BCAm}} [\text{mol}/\text{L}] = 1.21 \times 10^{-4} a \quad (1)$$

where  $a$  is the absorbance at 255 nm and  $C_{\text{BCAm}}$  is the concentration of poly-BCAm. The concentration of BCAM in poly-NIPAM-*co*-BCAm was estimated using eq 1.



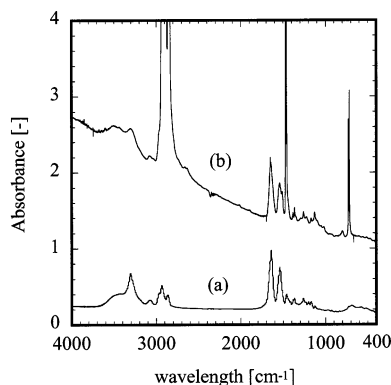


**Figure 4.** IR spectra of (a) poly-NIPAM-co-BCAm and (b) PE-g-NIPAM-co-BCAm.

The quantity of crown ether receptors contained in PE-g-NIPAM-co-BCAm could not be determined directly from UV measurements; we therefore determined it using IR measurements. Figure 4 shows the IR spectra of poly-NIPAM-co-BCAm and PE-g-NIPAM-co-BCAm. The IR absorbance ratio of the peak at  $1388\text{ cm}^{-1}$ , from the isopropyl group of NIPAM, to that at  $1133\text{ cm}^{-1}$ , from the ether group of the BCAM, is related to the copolymerization ratio of NIPAM to BCAM determined using eq 1, as follows:

$$y[-] = 4.6 \times 10^2 h_{\text{BCAm/NIPAM}} \quad (2)$$

where  $y$  is the copolymerization ratio of NIPAM and BCAM determined by UV-vis and  $h_{\text{BCAm/NIPAM}}$  is the IR absorbance ratio of the peak heights at  $1388\text{ cm}^{-1}$ :  $1133\text{ cm}^{-1}$ . The copolymerization ratio of NIPAM to BCAM was determined to be 93:7 using eq 2.

**Quantity of Crown Ether Receptors Contained in PE-g-NIPAM-co-BCAm from Measurement of the Adsorbed Ions.** This quantity was also determined by measuring the adsorbed ions. Assuming that the crown ether receptors form 1:1 complexes with the ions, then the complex formation constant of the crown ether receptor is defined as

$$K = \frac{[\text{HG}]}{[\text{H}][\text{G}]} \quad (3)$$

where  $[\text{H}]$  is the concentration of the crown ether receptors that do not form the complexes,  $[\text{G}]$  is the concentration of the ions, and  $[\text{HG}]$  is the concentration of the complexes. Equation 3 was transformed into the following equation:

$$\frac{1}{[\text{HG}]} = \frac{1}{K[\text{H}]_0[\text{G}]} + \frac{1}{[\text{H}]_0} \quad (4)$$

where  $[\text{H}]_0$  is the total concentration of the crown ether receptors. Figure 5 shows the relationship between  $1/[\text{HG}]$  and  $1/[\text{G}]$ ; by applying eq 4 to Figure 5,  $[\text{H}]_0$  was calculated to be 0.08 M.

However, FT-IR absorbance of PE-g-NIPAM indicated the amount of grafted NIPAM. This relationship is as follows:

$$h_{\text{NIPAM/PE}} = 0.19 W_{\text{NIPAM}} \quad (5)$$

where  $h_{\text{NIPAM/PE}}$  is the IR absorbance ratio of the peak at  $1388\text{ cm}^{-1}$  to that at  $1462\text{ cm}^{-1}$  and  $W_{\text{NIPAM}}$  [mg/cm<sup>2</sup>]

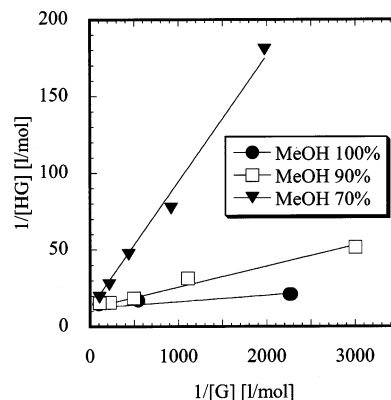


**Figure 5.** Relationship between the quantity of ion adsorption of the crown receptor,  $[\text{HG}]$ , and ion concentration of the bulk solution,  $[\text{G}]$ . KCl was used as an inorganic salt. The adsorption experiments were performed at  $25\text{ }^\circ\text{C}$  in a bulk solution of a mixture of methanol and water. The lines are fitted to eq 6.

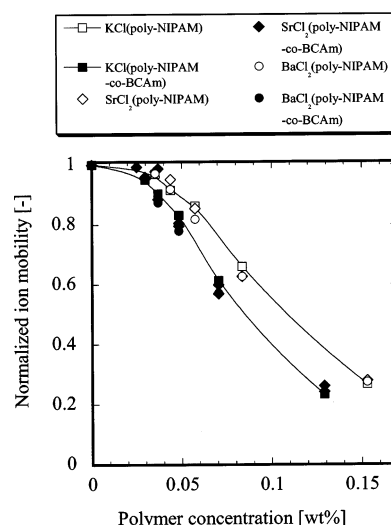


**Figure 6.** Ionic mobilities in aqueous poly-NIPAM-co-BCAm and ion solutions, as measured by an impedance analyzer at  $25\text{ }^\circ\text{C}$ . These values were normalized to be divided by the ionic mobilities of the corresponding aqueous ions.

is the amount of grafted poly-NIPAM. The amount of NIPAM was calculated to be 1.10 M using eq 5.

Consequently, the copolymerization ratio of NIPAM:BCAM was 93:7, which was compatible with the ratio determined by spectroscopic methods.

**Complex Formation Constant (log  $K$ ) of the Crown Ether Receptors.** For the crown ether receptors contained in PE-g-NIPAM-co-BCAm in a mixture of methanol and water, this constant had been already calculated for  $[\text{H}]_0$  as shown in Figure 5. Log  $K$  decreased with decreasing methanol ratio. At methanol ratios below 70 wt %, log  $K$  was too small to be determined by adsorption measurement. Therefore, it was necessary to determine log  $K$  in pure water by another method.

Accordingly, assuming that log  $K$  of the receptors of both PE-g-NIPAM-co-BCAm and poly-NIPAM-co-BCAm are equal, we determined the log  $K$  of the crown ether receptors contained in poly-NIPAM-co-BCAm in pure water. Instead of the ion adsorption measurement described above, we used the ionic mobility measurement. Figure 6 shows the ionic mobilities of poly-NIPAM-co-BCAm and poly-NIPAM aqueous ionic solutions, which were normalized to the ionic mobilities of

**Table 1. Complex Formation Constants of the Crown Ether of Poly-NIPAM-co-BCAm with Various Ions in Water**

ion	log $K^a$ of crown ether receptor of poly-NIPAM-co-BCAm	log $K^b$ of benzo[18]crown-6
K <sup>+</sup>	1.0	1.84
Sr <sup>2+</sup>	1.1	2.41 <sup>c</sup>
Ba <sup>2+</sup>	1.6	2.90 <sup>c</sup>

<sup>a</sup> As measured using an impedance analyzer. <sup>b</sup> As cited in: Izatt, M. R.; Pawlak, K.; Bradshaw, S. J. *Chem. Rev.* **1991**, *91*, 1721.  
<sup>c</sup> With NO<sub>3</sub><sup>-</sup> anions.

the corresponding aqueous ionic solutions that did not contain any polymer. The ionic mobility of poly-NIPAM-co-BCAm was smaller than that of poly-NIPAM. Assuming that any ion-hopping effect on the conductivity is negligible, decreases in ionic mobility arise from the capture of ions by the crown ether receptors. This assumption is appropriate for two reasons: (i) the concentration of the copolymer is low, and (ii) the BCAm ratio in the copolymer is as low as 7 mol %. The distance between the crown ether receptors is so great that no ion hopping can occur.

Accordingly, [G] was determined using the normalized ion mobility. [G] can be expressed by eq 6, which is derived from eq 4 using [H]<sub>0</sub> and [G]<sub>0</sub>. [HG] can be eliminated using the initial concentration of the ions, [G]<sub>0</sub>, because of the relationship [G]<sub>0</sub> = [HG] + [G].

$$[G] =$$

$$-K\left([H]_0 + [G]_0 + \frac{1}{K}\right) + \sqrt{K^2\left([H]_0 - [G]_0 + \frac{1}{K}\right)^2 + 4K[G]_0} \quad (6)$$

The values of [G] can be determined from the normalized ionic mobility using the least-squares method to fit to eq 6.  $K$  was then calculated as shown in Table 1.

All the log  $K$  values measured by ion adsorption or ionic mobility are summarized in Figure 7. In pure water, log  $K$  of the crown ether receptor was less than two. This value of log  $K$  is smaller than that of benzo[18]crown-6, and hence, log  $K$  was greatly reduced by polymerization. As a consequence, the capturing ability of the crown ether receptor of the molecular recognition polymer decreased compared with benzo[18]crown-6 in water, methanol, or in a mixture of water and methanol.

Previous studies have reported that the capturing ability of the crown ether receptor was increased by polymerization. Smid et al.<sup>23</sup> measured the capturing ability of poly(vinylbenzo[18]crown-6) and vinylbenzo[18]crown-6 in CHCl<sub>3</sub> by picric salt extraction, and Kimura et al.<sup>24</sup> also measured the capturing ability of BCAm, bis-BCAm, and poly-BCAm in CHCl<sub>3</sub> by picric salt extraction. These observed increases in log  $K$  were caused by the formation of a 2:1 sandwich complex in addition to the 1:1 complex. However, in our study, the BCAm ratio in poly-NIPAM-co-BCAm was as low as 7 mol %; therefore, the distances between crown ether receptors were so great that the crown ether receptors could only form the 1:1 complex. In addition, conformation of the crown ether receptor was restricted by polymerization, and therefore, log  $K$  of crown ether receptors of the BCAm units was much smaller than that for benzo[18]crown-6.

**Relationship between DSC Measurement and the Membrane Response Function.** Both LCST and

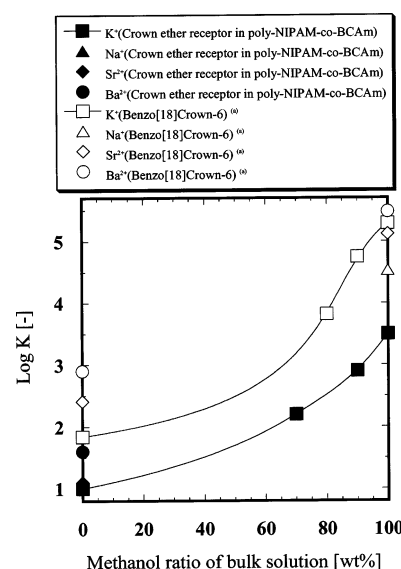


**Figure 7.** Log  $K$  of the crown ether receptor of the copolymer of NIPAM and BCAm and of benzo[18]crown-6 in a mixture of water and methanol at 25 °C. The adsorption measurement could not determine log  $K$  of the receptor in pure water. Therefore, log  $K$  of poly-NIPAM-co-BCAm in pure water was measured using the impedance analyzer. Log  $K$  of benzo[18]crown-6 (see (a)) was cited from: Izatt, R. M.; Pawlak, K.; Bradshaw, J. S. *Chem. Rev.* **1991**, *91*, 1721–2085.

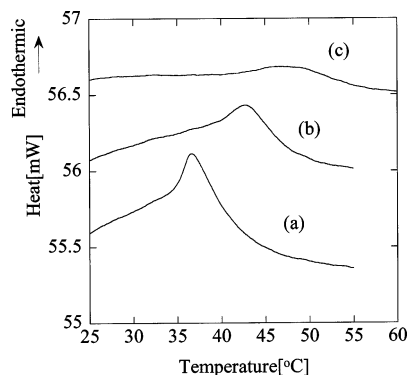


**Figure 8.** Dependency of the DSC thermograms on the Sr<sup>2+</sup> concentration: (a) 0.01, (b) 0.04, and (c) 0.1 M.

$\Delta H$  with phase transition were determined using DSC measurement. LCST is defined as the temperature at the peak of the DSC thermogram.  $\Delta H$  was determined from the area of the peak of the DSC thermogram. Figure 8 shows the DSC thermogram of the phase transition of PE-*g*-NIPAM-co-BCAm. The LCST shifted to higher temperatures with increasing Sr<sup>2+</sup> concentration. At the same time,  $\Delta H$  decreased and the peak broadened.

The LCST determined by DSC data represented the LCST of phase transition. Figure 9 shows the relationship between LCST determined by DSC and LCST determined by filtration, which was defined as the temperature when the pure water permeability ( $L_p$ ) was  $5 \times 10^{-5} \text{ m}^3 \text{ m}^{-2} \text{ s}^{-1} (\text{kgf/cm}^2)^{-1}$ . This  $L_p$  value was 16% of the  $L_p$  value when all the pores of the gating membrane were opened.<sup>3</sup> The LCST measured by DSC represents the volume change of grafted copolymer and the filtration response function; we can therefore estimate the temperature at which the membrane opens using the LCST determined by DSC.

**LCST Shift Caused by Complex Formation by the Crown Ether Receptors and Ions.** We investi-

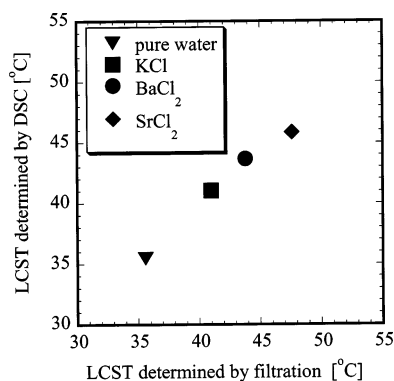


**Figure 9.** Relationship between LCST measured by DSC and LCST measured by filtration experiments. LCST measured by DSC was defined by the temperature at the top of DSC curve, and LCST determined by filtration was defined as the temperature at which the pure water permeability flux ( $L_p$ ) was  $5 \times 10^{-5} \text{ m}^3 \text{ m}^{-2} \text{ s}^{-1} (\text{kgf/cm}^2)^{-1}$ .

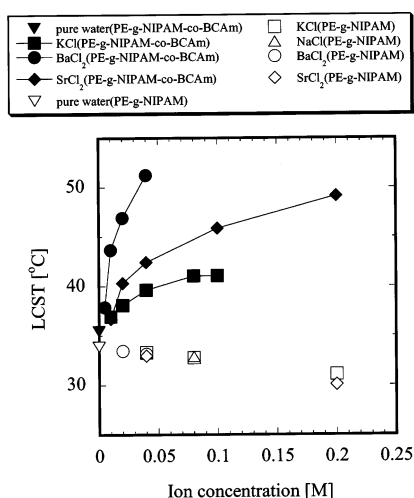


**Figure 10.** Dependency of the ion concentration on the LCST of PE-*g*-NIPAM-*co*-BCAm (open symbols) and PE-*g*-NIPAM (closed symbols), as measured by DSC. The LCST values were determined from the temperature of the peak maximum on the DSC thermograms.

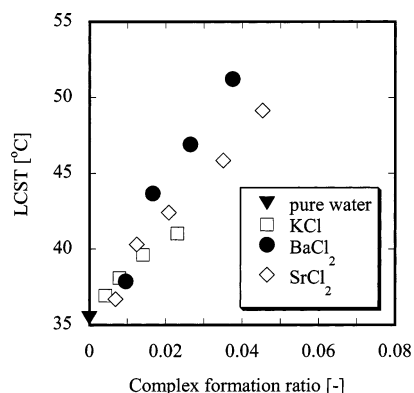


**Figure 11.** Relationship between the complex formation ratio and LCST, as measured by DSC.

gated the effect of the addition of various ions to the LCSTs of both PE-*g*-NIPAM-*co*-BCAm and PE-*g*-NIPAM. Figure 10 shows the relationship between LCST and the initial ion concentration of the solution in which PE-*g*-NIPAM-*co*-BCAm and PE-*g*-NIPAM were immersed. The LCST of PE-*g*-NIPAM slowly shifted to lower temperatures with the addition of any kind of cation. This result is compatible with a cross-linked gel of

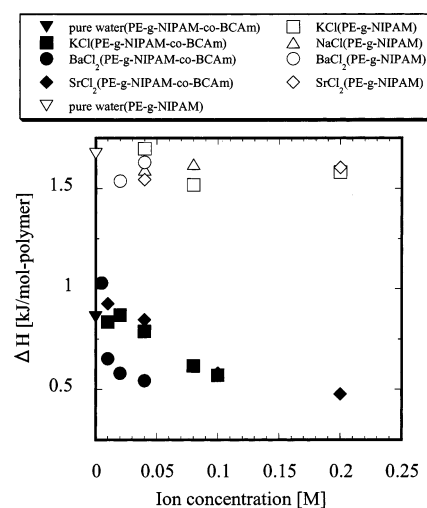


**Figure 12.** Dependency of the ion concentration on  $\Delta H$  of PE-*g*-NIPAM-*co*-BCAm (open symbols) and PE-*g*-NIPAM (closed symbols), as measured by DSC.  $\Delta H$  is the molar heat; the measured value was divided by the number of moles of BCAM and NIPAM monomer units contained in the copolymer.

NIPAM<sup>25</sup> and can be explained by a salting-out effect. However, the LCST of PE-*g*-NIPAM-*co*-BCAm showed a large shift to higher temperatures with the addition of a cation. Furthermore, the order of LCST shift was  $\text{Ba}^{2+} > \text{Sr}^{2+} > \text{K}^+$  when the ion concentrations were the same. This order coincided with the order of  $\log K$  of the crown ether receptors.  $\log K$  determines the quantity of the complex of the crown ether receptors and ions; thus, the quantity of the complex might cause the LCST shift.

To discuss the quantity of the complex, we defined the complex formation ratio ( $X$ ) as the ratio of the quantity of BCAM units that form complexes with ions ( $\text{unit}_{\text{complexingBCAM}} = [\text{HG}]$ ) to the total quantity of monomer units ( $\text{unit}_{\text{NIPAM}} + \text{unit}_{\text{BCAM}}$ ) as follows:

$$X = \frac{[\text{HG}]}{\text{unit}_{\text{NIPAM}} + [\text{H}]_0} = \frac{\text{unit}_{\text{complexingBCAM}}}{\text{unit}_{\text{NIPAM}} + \text{unit}_{\text{BCAM}}} \quad (7)$$

$X$  was determined from the added ion concentration and  $\log K$ , as shown in Table 1. Figure 11 shows the relationship between LCST and  $X$ ; this relationship was linear and did not depend on the species of ion. Therefore, the important factor in the LCST shift was  $X$ , which expresses the quantity of the complex.

**Effect of Complex Formation by the Crown Ether Receptors and Ions on  $\Delta H$  Decrease.**  $\Delta H$  values for PE-*g*-NIPAM-*co*-BCAm and PE-*g*-NIPAM are shown in Figure 12.  $\Delta H$  of PE-*g*-NIPAM-*co*-BCAm was about two-thirds of that of PE-*g*-NIPAM in pure water. As shown in previous studies,<sup>10,22</sup> breakage of hydrogen bonds between the water molecules that surround the hydrophobic moieties of polymer chains is the main contributor to  $\Delta H$ . This increase of entropy of water molecules is compensated by the endothermic enthalpy change,<sup>17a</sup> which was measured by DSC. This breakage of hydrogen bonds was measured directly using Raman spectroscopic measurements.<sup>18b,c</sup> Interpreting the decrease of  $\Delta H$  from PE-*g*-NIPAM to PE-*g*-NIPAM-*co*-BCAm on the basis of these previous studies, breakage of hydrogen bonds between the water molecules that surround the hydrophobic moieties of polymer chains occurred in pure water by introducing BCAM units into the NIPAM chain.

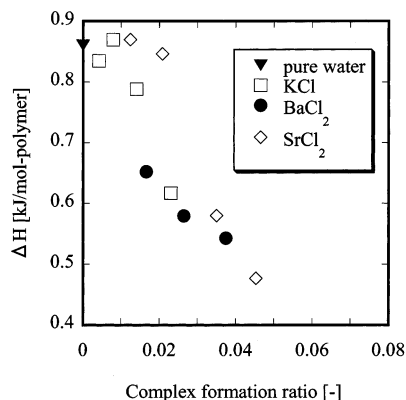


**Figure 13.** Relationship between the complex formation ratio and  $\Delta H$ , as measured by DSC.

The  $\Delta H$  change with ion concentration of PE-*g*-NIPAM-*co*-BCAm was also different from that for PE-*g*-NIPAM, as shown in Figure 12.  $\Delta H$  of PE-*g*-NIPAM remained constant, regardless of ion concentration. In contrast,  $\Delta H$  of PE-*g*-NIPAM-*co*-BCAm decreased with increasing ion concentration. This means that the breakage of hydrogen bonds between the water molecules that surround the hydrophobic moieties of polymer chains increased when the crown ether receptors caught the ions and formed the complex. However, the slope of the decrease in  $\Delta H$  was different for each ion, and thus we considered the relationship between  $\Delta H$  and  $X$  in the same way as LCST, as shown in Figure 13.  $\Delta H$  decreased linearly with increasing  $X$ , regardless of the ion species. Therefore, the breakage of the hydrogen bonds was determined only by the quantity of the complex with the receptors and the ions.

**Mechanism of Phase Transition of PE-*g*-NIPAM-*co*-BCAm.** Given the above considerations, the mechanism of the phase transition of PE-*g*-NIPAM-*co*-BCAm is as follows. The formation of the complexes of crown ether receptors and ions breaks hydrogen bonds between the water molecules that surround the hydrophobic moieties of polymer chains in the swelling state; hence, the entropy change with phase transition decreases when the copolymer chain shrinks. Consequently, the entropy change does not require a large compensating endothermic  $\Delta H$  change, and  $\Delta H$  thus decreases with complex formation.

The mechanism of LCST shift can be explained in the same way. Generally, hydrogen bonding of water molecules is gradually broken with increasing temperature. This breakage triggers the breakage of hydrogen bonds surrounding the hydrophobic moieties of polymer chains at the LCST. However, by the formation of the complexes, this hydrogen bonding around the hydrophobic moieties has already broken in the swelling state before the phase transition occurs. Accordingly, the copolymer that forms the complex does not shrink at the LCST of pure water, but maintains the swelling condition, and then shrinks at higher temperatures.

From this mechanism, it is predicted that the LCST will shift to higher temperatures when  $\Delta H$  decreases. Figure 14 shows the inverse relationship between LCST and  $\Delta H$ ; this result coincides with the suggested mechanism. This suggested mechanism is also strongly supported by  $\Delta H$  measurement results for poly-NIPAM-*co*-vinylimidazole (VIm).<sup>9c</sup> VIm has a positive charge; therefore, the introduction of VIm causes similar phenomena to the complex formation of BCAm. When the

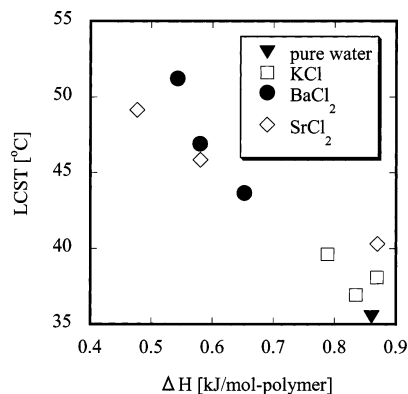


**Figure 14.** Relationship between LCST and  $\Delta H$ , as measured by DSC.

VIm ratio increases, LCST shifts higher and  $\Delta H$  decreases, so that the LCST has an inverse relation with  $\Delta H$ .

The interesting and important point of the suggested mechanism is that the breakage of hydrogen bonds did not depend on ion species but on  $X$ . This means that both the hydration of the complex and the breakage effect of hydrogen bonding of the complex also did not depend on the ion species. Samoilov<sup>26</sup> divided ions into two categories, positive hydrated ions and negative hydrated ions, on the basis of the activation energy required for water molecules to move into bulk solution from the vicinity of the ions. However, the ions captured by crown ethers were restricted to contact with the water molecules by coordination bonds with the oxygen atoms of the crown ethers.<sup>27</sup> Thus, the hydration structure of the complex of the crown ether receptor and ion is almost the same, regardless of ion species. The size of the cluster containing the complex and hydration water molecules was estimated using DSC measurements at low temperatures near 0 °C;<sup>28</sup> these results supported the suggested phase transition mechanism.

## Conclusions

A molecular recognition ion gating membrane opens and closes its pores using the volume phase transition of PE-*g*-NIPAM-*co*-BCAm, which recognizes specific ions by its BCAm receptors and changes its volume with swelling and shrinking. We have clarified the mechanism of molecular recognition response of the PE-*g*-NIPAM-*co*-BCAm. The crown ether receptor in BCAm of the copolymer formed the complex with the specific ion. However, the complexed BCAm units to total monomer units ( $X$ ) were slightly below 5%. This small amount of the complexes broke the hydrogen bonds. This breakage of hydrogen bonds did not depend on ion species but on  $X$ ; this means that the hydration and hydrogen bond breakage effects of the complex are almost the same, regardless of ion species. The suggested mechanism will contribute both to the molecular design of grafted copolymers and to the design of the gating membrane function in the future.

## References and Notes

- (1) (a) Mika, A. M.; Childs, R. F.; Dickson, J. M.; McCarry, B. E.; Gagnon, D. R. *J. Membr. Sci.* **1995**, *108*, 37. (b) Ishihara, K.; Kobayashi, M.; Shinohara, I. *Macromol. Chem. Rapid Commun.* **1983**, *4*, 327. (c) Miyata, T.; Asami, N.; Uragami, T. *Nature (London)* **1999**, *399*, 766. (d) Baker, J. P.; Siegel, R. A. *Macromol. Chem. Rapid Commun.* **1996**, *17*, 409.



- (2) Yamaguchi, T.; Ito, T.; Sato, T.; Shinbo, T.; Nakao, S. *J. Am. Chem. Soc.* **1999**, *121*, 4078.
- (3) Ito, T.; Hioki, T.; Yamaguchi, T.; Shinbo, T.; Nakao, S.; Kimura, S. *J. Am. Chem. Soc.* **2002**, *124*, 7840.
- (4) Chu, L.-Y.; Yamaguchi, T.; Nakao, S. *Adv. Mater.* **2002**, *14*, 386.
- (5) Hirokawa, Y.; Tanaka, T. *J. Chem. Phys.* **1984**, *81*, 6379.
- (6) Irie, M.; Misumi, Y.; Tanaka, T. *Polymer* **1993**, *34*, 4531.
- (7) Aoki, T.; Muramatsu, M.; Torii, T.; Sanui, K.; Ogata, N. *Macromolecules* **2001**, *34*, 3118.
- (8) Coles, C. A.; Schreinder, S. M.; Priest, J. H.; Monji, N.; Hoffman, A. S. *ACS Symp. Ser.* **1987**, *350*, 245.
- (9) (a) Maeda, Y.; Higuchi, T.; Ikeda, I. *Langmuir* **2001**, *17*, 7535. (b) Maeda, Y.; Nakamura, T.; Ikeda, I. *Macromolecules* **2001**, *34*, 1391. (c) Maeda, Y.; Yamamoto, H.; Ikeda, I. *Langmuir* **2001**, *17*, 6855.
- (10) Schild, H. G.; Tirrel, D. A. *J. Phys. Chem.* **1990**, *94*, 4352.
- (11) Lin, S.-Y.; Chen, K.-S.; Liang, R.-C. *Polymer* **1999**, 2619.
- (12) Kawasaki, H.; Sasaki, S.; Maeda, H. *Langmuir* **2000**, *16*, 3195.
- (13) (a) Torres-Lugo, M.; Peppas, N. A. *Macromolecules* **1999**, *32*, 6646. (b) Khare, A. R.; Peppas, N. A. *Polymer* **1993**, *34*, 4736.
- (14) (a) Shibayama, M.; Mizutani, S.; Nomura, S. *Macromolecules* **1996**, *29*, 2019. (b) Suetoh, Y.; Shibayama, M. *Polymer* **2000**, *41*, 505.
- (15) Schonhoff, M.; Larsson, A.; Welzel, P. B.; Kuckling, D. *J. Phys. Chem. B* **2002**, *106*, 7800.
- (16) Grinberg, N. V.; Dubovik, A. S.; Grinberg, V. Y.; Kuznetsov, D. V.; Makhaeva, E. E.; Grosberg, A. Y.; Tanaka, T. *Macromolecules* **1999**, *32*, 1471.
- (17) (a) Tokuhira, T.; Amiya, T.; Mamada, A.; Tanaka, T. *Macromolecules* **1991**, *24*, 2936. (b) Ray, S. S.; Rajamohanam, P. R.; Badiger, M. V.; Devotta, I.; Ganapathy, S.; Mashelkar, R. A. *Chem. Eng. Sci.* **1998**, *53*, 869.
- (18) (a) Suzuki, Y.; Suzuki, N.; Takatsu, Y.; Nishio, I. *J. Chem. Phys.* **1997**, *107*, 5890. (b) Maeda, Y.; Tsukida, N.; Kitano, H.; Terada, T.; Yamanaka, J. *J. Phys. Chem.* **1993**, *97*, 13903. (c) Maeda, Y.; Kitano, H. *Spectrochim. Acta A* **1995**, *51*, 2433.
- (19) Winnik, F.-M. *Macromolecules* **1990**, *23*, 233.
- (20) (a) Ungaaro, R.; El Haj, B.; Smid, J. *J. Am. Chem. Soc.* **1976**, *98*, 5198. (b) Yagi, K.; Ruitz, J. A.; Sanchez, M. C. *Macromol. Chem. Rapid Commun.* **1980**, *1*, 263.
- (21) Yamaguchi, T.; Nakao, S.; Kimura, S. *Macromolecules* **1991**, *24*, 5522.
- (22) Otake, K.; Inomata, H.; Kono, M.; Saito, S. *Macromolecules* **1990**, *23*, 283.
- (23) Kopolow, S.; Hogen Esch, T. E.; Smid, J. *Macromolecules* **1971**, *4*, 359.
- (24) Kimura, K.; Maeda, T.; Shono, T. *Talanta* **1979**, *26*, 945.
- (25) (a) Suzuki, A. *Adv. Polym. Sci.* **1993**, *110*, 199. (b) Inomata, H.; Goto, S.; Otake, K.; Saito, S. *Langmuir* **1992**, *8*, 687.
- (26) (a) Samoilov, O. Y. *Discuss. Faraday Soc.* **1957**, *24*, 141. (b) Chong, S.-H.; Hirata, F. *J. Phys. Chem. B* **1997**, *101*, 3209.
- (27) (a) Ozutsumi, K.; Natsuhara, M.; Ohataki, H. *Bull. Chem. Soc. Jpn.* **1989**, *62*, 2807. (b) Raghino, G.; Romano, S.; Lehn, J. M.; Wipff, G. *J. Am. Chem. Soc.* **1985**, *107*, 7873.
- (28) Ito, T.; Nishikawa, M.; Yamaguchi, T. Manuscript in preparation.

MA030590W